NEW EXPERIMENTAL FINDINGS ON THE STABILITY OF THIN REINFORCED CONCRETE WALLS

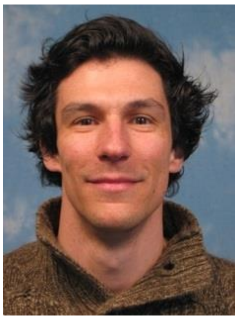


João P. Almeida*
Investigador de Pós-Dout.
EESD Lab, EPFL
Lausanne, Suiça
joao.almeida@epfl.ch

Angelica Rosso
Aluna de Doutoramento
EESD Lab, EPFL
Lausanne, Suiça
angelica.rosso@epfl.ch

Katrin Beyer
Professora Auxiliar
EESD Lab, EPFL
Lausanne, Suiça
katrin.beyer@epfl.ch

Sri Sritharan
Professor Catedrático
Iowa State University
Ames, Iowa, US
sri@iastate.edu

SUMMARY

Damage to structural walls in the recent earthquakes in Chile (2010) and New Zealand (2011) demonstrated that modern reinforced concrete (RC) walls may not achieve the expected ductile response and these walls could possibly fail due to global and local buckling.

This paper describes the experimental test of an extensively instrumented thin RC wall subjected to in-plane loading. However, the wall experienced significant out-of-plane deformations, which ultimately triggered member failure at the local level. Through a detailed evaluation of measured experimental data including that collected from optical sensors, the observed wall performance is more accurately realized.

Finally, suggestions for improving existing phenomenological wall models for out-of-plane behaviour and the corresponding numerical simulation tools are provided.

Keywords: Out-of-plane instability, Thin RC walls, Large-scale cyclic tests, Numerical modelling, Buckling

1. INTRODUCTION

Recent earthquakes in Chile (2010, Mw 8.8) and New Zealand (2011, M 6.3) have shown that, despite many years of extensive research and subsequent design code advancements, many reinforced concrete (RC) walls underperformed during these seismic events. In fact, many of these structural failures are not yet completely understood [1]. In some cases lateral instability of large portion of walls was detected—see Figure 1(a)—which corresponds to a buckling type of failure that had been observed primarily in laboratory tests [2]. These issues deserve thorough investigations to ensure their satisfactory performance in future earthquakes.

Figure 1(b) shows buckling of one leg of an L-shaped shear wall in a 7-story building constructed during the mid-1980s in Christchurch. The wall buckled over a height of approximately 1 m and crushing extended over 3 m into the web. Comparable damage was also observed after the Chile earthquake, which was characterized by longer duration and several large intensity cycles [3]. The performance of these walls, therefore, suggests that the limits on slenderness required in the current codes may not be sufficient to prevent wall buckling; research is thus required to better understand this phenomenon and improve the design codes accordingly.

An ongoing series of experimental cyclic tests on thin RC walls, comprehensively instrumented, is being carried out at the *Earthquake Engineering and Structural Dynamics Laboratory* of EPFL, Switzerland. This paper presents the results obtained from the first wall test, and of the advances that it brings to the current knowledge on wall instability, both in terms of understanding of the phenomenon and consequences for mathematical simulation.

(a)

(b)

Figure 1. Examples of out-of-plane induced damages in RC walls after: (a) Chile earthquake [4]; (b) New Zealand earthquake [5,6].

Following a review of the main features of the physical development of out-of-plane member buckling and past modelling efforts, this paper briefly describes the experimental programme in progress and summarises the behaviour of the first wall test. Post-processed experimental measurements are then discussed and compared with observations reported by previous researchers. Emphasis is placed on the identification of novel findings that question accepted hypotheses, and on their consequences for improving the modelling techniques.

2. DESCRIPTION OF WALL INSTABILITY AND EXISTING MODELS

A limited number of pioneering works on out-of-plane stability of RC walls considering in-plane loading have been published over the last decades, e.g. Paulay and Priestley [7] and Chai and Elayer [8]. Such studies describe the basic mechanics of the phenomenon, identify some of the fundamental features triggering a potentially unstable wall behaviour, and propose simple phenomenological models. Very recently, following the above mentioned occurrences in earthquake-struck regions, researchers have refocused their attention on this deformation mode, its effects on member failure, and advanced simulation techniques [2].

2.1 Mechanics of out-of-plane buckling

Paulay and Goodsir [9,10] were the first to describe the development of out-of-plane mechanism for thin concrete walls. Using a wall with double layer reinforcement as in Figure 2, this mechanism can be summarised as follows [7]. At large in-plane curvature demands, the wall bottom corner region develops large tensile strains that cause wide near-horizontal cracks across the width of the section. That leads to longitudinal reinforcement yielding in tension and followed by strain-hardening. Upon unloading, an elastic strain recovery takes place, although the cracks remain open due to the plastic tensile strains previously accumulated in the rebars. During reloading in compression, and until crack closure, the compression force must be resisted solely by the two layers of vertical reinforcement. This stage is typically accompanied by an incipient out-of-plane displacement, which occurs due to construction misalignments in the position of the longitudinal reinforcements or eccentricity of the axial force C acting in this region, see Figure 2(b). While the rebars retain their significant axial stiffness before yielding in compression, the out-of-plane displacement tends to remain small. However, as compression increases the longitudinal rebar near the concave side (intrados of the out-of-plane deformed profile) can potentially yield, originating an abrupt reduction in stiffness and a consequent increase in the out-of-plane displacement. It is noted that, at this point, the second layer of longitudinal reinforcement—which has not yet yielded in compression—is the main source of out-of-plane stiffness. Such restraint does not even show up for RC walls with a single layer of reinforcement, when the only rebar layer attains compressive yielding and the crack is still fully open.

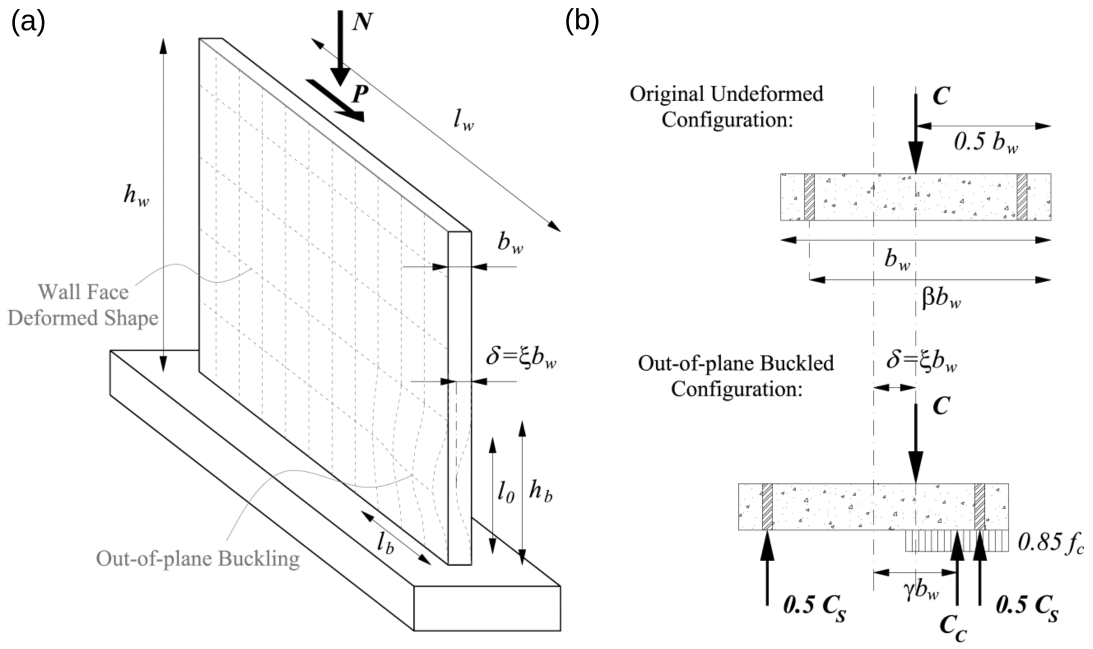

Figure 2. (a) Wall geometrical characterization; (b) Equilibrium of external and internal forces at mid-height of buckling region, adapted from Paulay and Priestley [6].

Depending on the magnitude of the tensile strain previously attained (i.e., before unloading), different scenarios can then take place as compression progresses. The cracks may close, re-establishing compressive force transfer through concrete, or they may remain open leading to compression yielding of the second layer of reinforcement. In the latter case, out-of-plane displacements will abruptly increase, leading to wall buckling failure. Intermediate conditions, wherein the second layer of reinforcement yields but cracks still close, at least partially, are also possible. Independently of the scenario that effectively takes place, the occurrence of out-of-plane displacements and second-order moments will affect the in-plane wall response and should therefore be taken into account [7].

In view of the above description, it is not surprising that the potential for out-of-plane buckling of thin walls depends foremost on the maximum inelastic tensile strain on the vertical wall edge regions, which has been since adopted as indicator of lateral stability of walls [7,8].

2.2 Brief review of existing models

The mechanics of out-of-plane buckling reported in the previous section also explains why the lateral stability of ductile RC walls subjected to in-plane seismic loading is usually investigated by considering the plastic hinge regions in the wall edges as an axially loaded column under large amplitude cyclic tension and compression. Existing phenomenological models are also based on this idealization. This configuration, with pin-ends at the extremities and length equal to the distance between the points of contraflexure in the buckled wall, has been adopted as well in most of the laboratory tests carried out in columns to gain understanding on lateral stability issues of walls.

To date, there are few indications on how to estimate or define the wall region that undergoes out-of-plane buckling—represented in Figure 2(a) by $l_b \times h_b$—and how the latter relates to the longitudinal reinforcement layout, in particular the presence of confined boundary elements. The influence of boundary conditions and the strain gradient throughout the cross-section is also lacking research, as well as the validation of expressions to compute the buckling length l_0. The previous wall-column idealization involves yet other relatively strong assumptions, affecting both models and experimental tests, which is discussed further in section 5.

This section briefly recalls and discusses some common assumptions of the existing phenomenological models on lateral stability of walls. Consider Figure 2(b), which depicts the internal forces at mid-height of the buckling length l_0 where the out-of-plane displacement $\delta=\xi b_w$ is larger. The total compression force C is taken by both the steel compression force C_S and the concrete compression force C_C, whose resultant is at an eccentricity γb_w. Assuming an equivalent rectangular compression stress block for the concrete compression force and that steel has reached its yield strength, vertical force and moment equilibrium produce:

$$\gamma = \frac{1}{2}\left[(\xi + 0.5) + \sqrt{(\xi + 0.5)^2 - 2\xi(1 + 1.176m)}\right] \tag{1}$$

where $m = \rho_b f_y / f_c$ is the mechanical reinforcement ratio of the wall strip of length l_b. This equation has real solutions only when the term inside the square root is non-negative:

$$\xi \le \xi_c = 0.5\left(1 + 2.35m - \sqrt{5.53m^2 + 4.7m}\right) \tag{2}$$

The previous equation represents the stability criterion of RC walls as derived by Paulay and Priestley [7]. The upper limit ξ_c is defined as the critical normalized out-of-plane displacement that marks the onset of wall instability.

The increase in arc length due to wall out-of-plane displacement results from the axial elongation of the wall strip over the buckling length l_0. Based on this assumption, Paulay and Priestley [7] and Chai and Elayer [8] established the following two relationships between the maximum average axial tensile strain over l_0 and the normalized out-of-plane displacement ξ_c:

$$\varepsilon_{sm,c} = 8\beta\left(\frac{b_w}{l_0}\right)^2 \xi_c \tag{3}$$

$$\varepsilon_{sm,c} = 8\beta\frac{\pi^2}{2}\left(\frac{b_w}{l_0}\right)^2 \xi_c + 3\varepsilon_y \tag{4}$$

According to both studies, l_0 may be taken as the equivalent plastic hinge length $l_p = 0.20l_w + 0.044h_w$. Paulay and Priestley [7] derived eq. (3) from geometrical considerations, where the parameter β takes into account the position of the vertical reinforcement within the wall thickness, as depicted in Figure 2(b). It is noted that β=0.5 for walls with a single layer of vertical reinforcement. Eq. (3), developed by Chai and Elayer [8], is a phenomenological equation based on tests of axially loaded concrete columns reinforced with two layers of vertical bars under large strains amplitudes. Therein, ε_y is the yield strain of the longitudinal reinforcement. This approach does not address the reduced out-of-plane stability expected for walls with a single layer reinforcement layout. The equations above should provide conservative predictions of a tensile strain below which crack closure, and subsequent crushing limit state, can be reached.

Capturing out-of-plane instability of RC walls through numerical models has been seldom attempted because of the challenges associated with the specificities of the nonlinear geometrical and material behaviour described above, as well as the lack of experimental data for comparison purposes. To the authors' knowledge, the only attempt to model the wall out-of-plane bulking was found in a recent study by Dashti et al. (2014).

3. EXPERIMENTAL PROGRAM

In order to experimentally study the lateral stability of walls, a test program consisting of five thin RC walls at 2/3-scale is in progress at the *Earthquake Engineering and Structural Dynamics Laboratory (EESD Lab)*, *École Polytechnique Fédérale de Lausanne (EPFL)*, Switzerland. The first three walls (TW1 to TW3) were tested using in-plane loads, while the last two specimens (TW4 and TW5) will be subjected to a combination of in-plane and out-of-plane direction loading. The geometrically identical walls TW1 and TW4 have the smallest wall thickness and the largest shear span ratio. Therefore, they are more prone to show instability issues. This paper analyses the results obtained from wall TW1, which was tested under a collaborative framework between the *EESD Lab* and the *School of Engineering of Antioquia* and the *University of Medellin*, in Colombia. The project was carried out with the purpose of evaluating seismic vulnerability of RC slender wall structures used for widespread construction of mid and high rise low-cost residential buildings in moderate and high seismic hazard zones in Colombia. It is noted that the Colombian construction code [11] does not impose a minimum wall thickness, unlike many other international codes. Figure 3 shows the dimensions and reinforcement details of wall TW1, representing the new wall design trend in Colombia.

The wall is 2000 mm tall, 80 mm wide and 2700 mm long, with a lateral flange 80 mm thick and 440 mm long. This short flange represents the effect of a perpendicular wall on member stability and damage distribution. Following a common Colombian detailing practice, the longitudinal reinforcement used a single layer of reinforcement, with 9 rebars d_w = 6 mm in the web, 3 rebars d_b = 16 mm in each boundary element, and 4 rebars d_w = 6 mm in the flange. The test unit had lap-splices at the bottom of the wall only for the bars with d_w = 6 mm in the web. The transverse reinforcement ratio consisted of d_t = 6 mm bars spaced at 200 mm. The foundation (3600 mm × 700 mm × 400 mm) was designed as a rigid support for the wall and rigidly connected to the strong floor with six prestressed bars. The concrete compressive strength is 28.8 MPa while its tensile strength is 2.2 MPa, as given by cylinder compression tests and double-punch tests, respectively. Rebar tensile tests showed yield / ultimate strengths of 460 / 625 MPa for the 6 mm bars, and 565 / 650 MPa for the 16 mm ones.

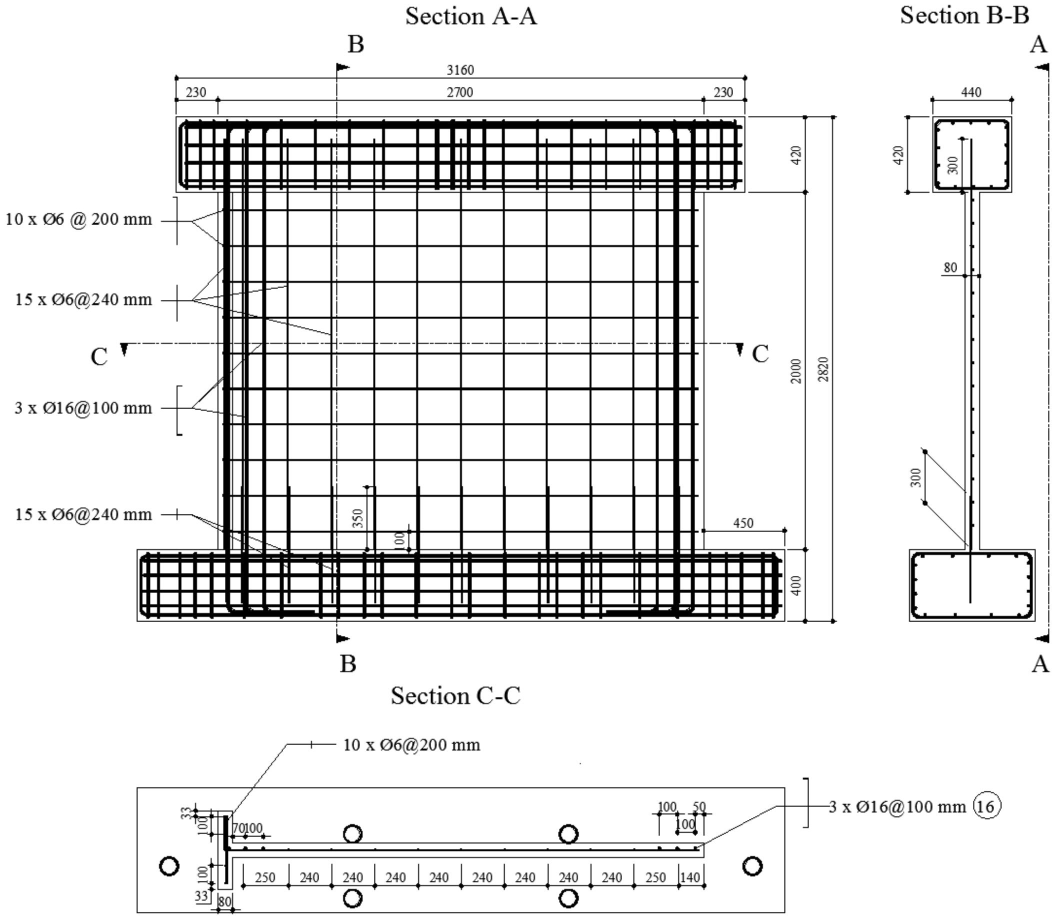

Figure 3. Geometrical characterization and detailing of test unit TW1.

An image and a sketch of the test setup are shown in Figure 4. A rigid steel beam was placed on the top of the RC beam, to warrant a distributed application of loads. Two vertical actuators were connected to the steel beam close to the wall ends to simulate simultaneously the axial load acting on the wall and the bending moment required to achieve the effects of a shear span of 10 m (corresponding to a shear span ratio of 3.7). A third horizontal actuator was connected to the top RC beam to simulate the in-plane loading. To restrain the out-of-plane displacements at the storey height, four steel tubes were placed at the height of the top RC beam to restrain the corresponding degrees of freedom, and the axial force in these tubes was checked with strain gage measurements. The loading protocol consisted of a reversed quasi-cyclic history, which was imposed by the horizontal actuator in displacement control. Two fully-reversed cycles were applied at each target drift, according to the following incremental drifts: ±0.05% $\rightarrow$ ±0.1% $\rightarrow$ ±0.15% $\rightarrow$ ±0.25% $\rightarrow$ ±0.35% $\rightarrow$ ±0.5% $\rightarrow$ ±0.75% $\rightarrow$ ±1%. A full description of the corresponding load stages can be observed in Figure 5.

As noted, the test unit was extensively instrumented. The instrumentation included eight vertical LVDTs positioned along the flange and web edges over the entire wall height, and one horizontal LVDT was used at the height of the top RC beam to record the imposed horizontal displacements. The in-plane and out-of-plane deformations of the wall surface were measured using a dense grid of 255 LEDs, represented in Figure 6, with the optical measurement system NDI Optotrak Certus HD [12]. Moreover, two corner regions of the wall—on the opposite wall face to where the markers were placed—were monitored using a digital imaging correlation system. Videos were made from different angles during the application of the load. At the end of each load stage photos were taken and progression cracking was traced and the widths of critical cracks were measured. A more detailed account of the experimental details and test observations can be found in Almeida et al. [13].

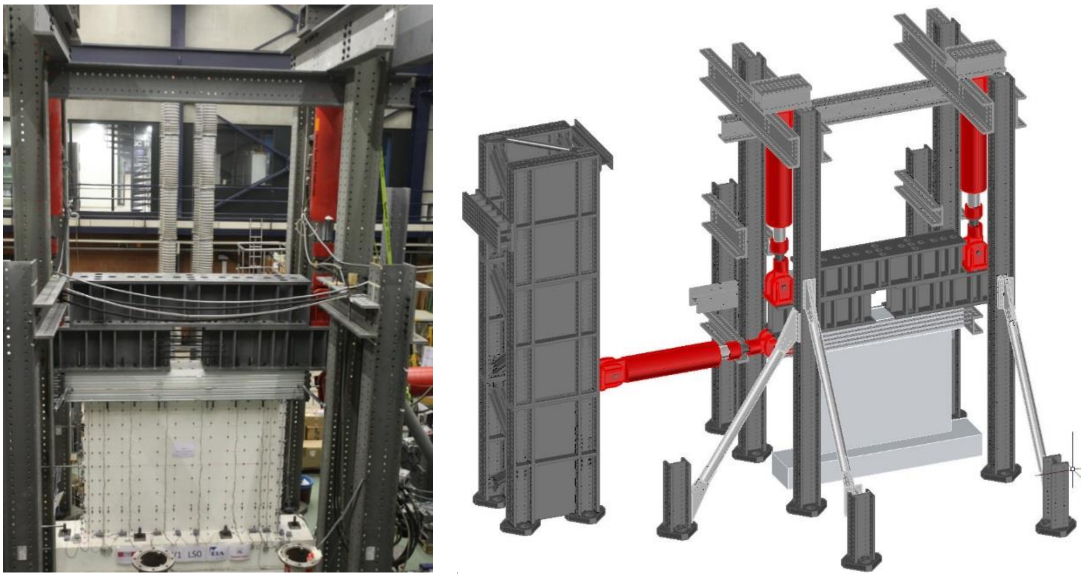

(a) (b)

Figure 4. Test setup in the *EESD Lab*: (a) Photo overview; (b) 3D representation.

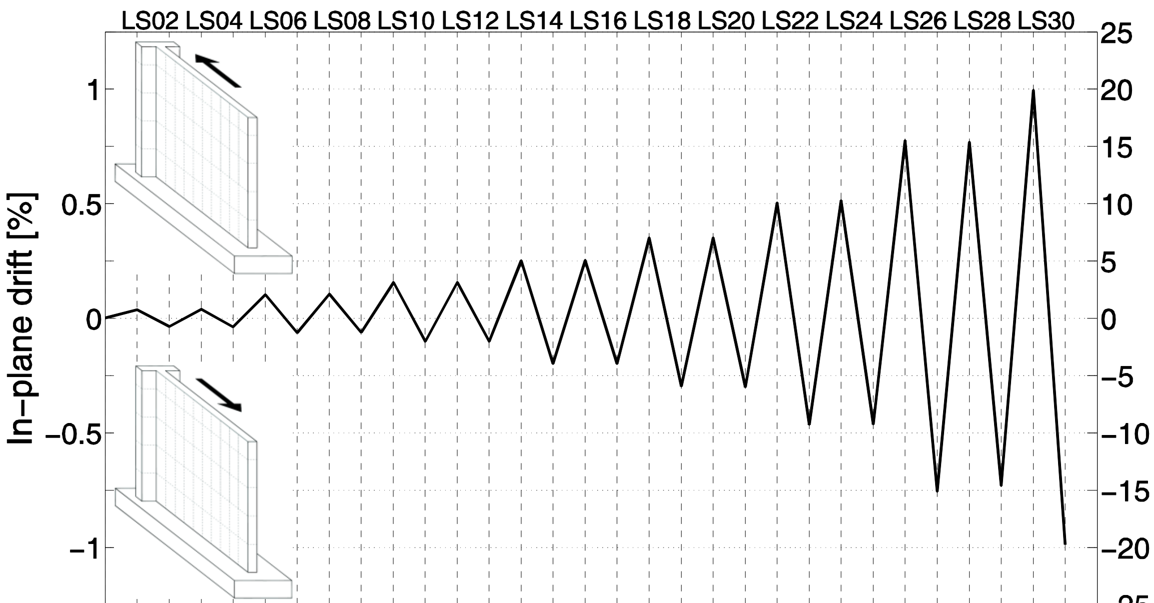

Figure 5. The load protocol used for TW1 with identification of load stages (LS).

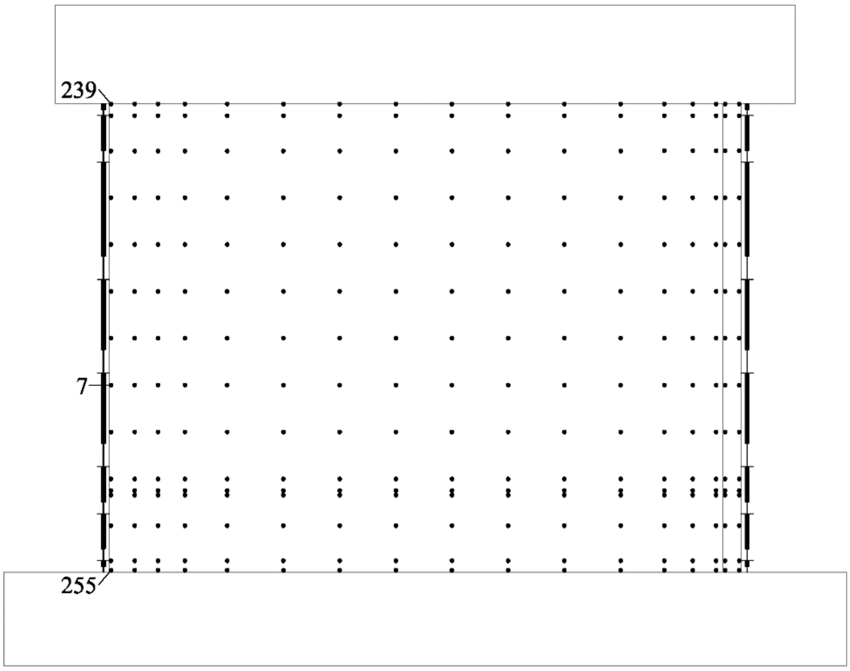

Figure 6. LED grid for the optical measurement system (with identification of LEDs #7, #239, and #255), and vertical LVDTs at wall edges.

4. SUMMARY OF TW1 RESULTS

This section discusses the main observations of the test of wall TW1, focusing on the out-of-plane response of the test unit. The in-plane force-displacement response of the member can be seen in Figure 7, which shows a stable hysteretic behaviour with appreciable dissipation of hysteretic energy. While loading from the flange to the web edges (i.e., towards negative values of drift in Figure 7), the wall showed clear signs of cyclic strength degradation from LS30 to LS31, when a drift of -1% was being targeted. During this loading, at a drift of -0.75%, the in-plane capacity of the wall was approximately 70% of the strength at cycle LS27 (also at -0.75% drift), which was followed soon after by a more sudden loss of load bearing capacity and corresponding failure of the test unit.

It is noted that the strength degradation that occurred during LS30→LS31 appears to have initiated during previous half-cycles when returning from positive drifts and approaching zero in-plane drift (where it was apparent that the force-displacement curve started to deviate from those corresponding to loadings LS26→LS27 and LS28→LS29). This strength degradation directly relates to the significant out-of-plane deformations that were observed along the height of the wall at 0% in-plane drift when loading towards negative drift values, see Figure 8(a). The plot in Figure 9(a), of the maximum out-of-plane displacement *versus* the wall in-plane displacement, clearly shows that the former is attained at around 0% in-plane drift, and not at the load stages corresponding to the maximum compression of the web edge (e.g., LS27, LS29), as one could expect.

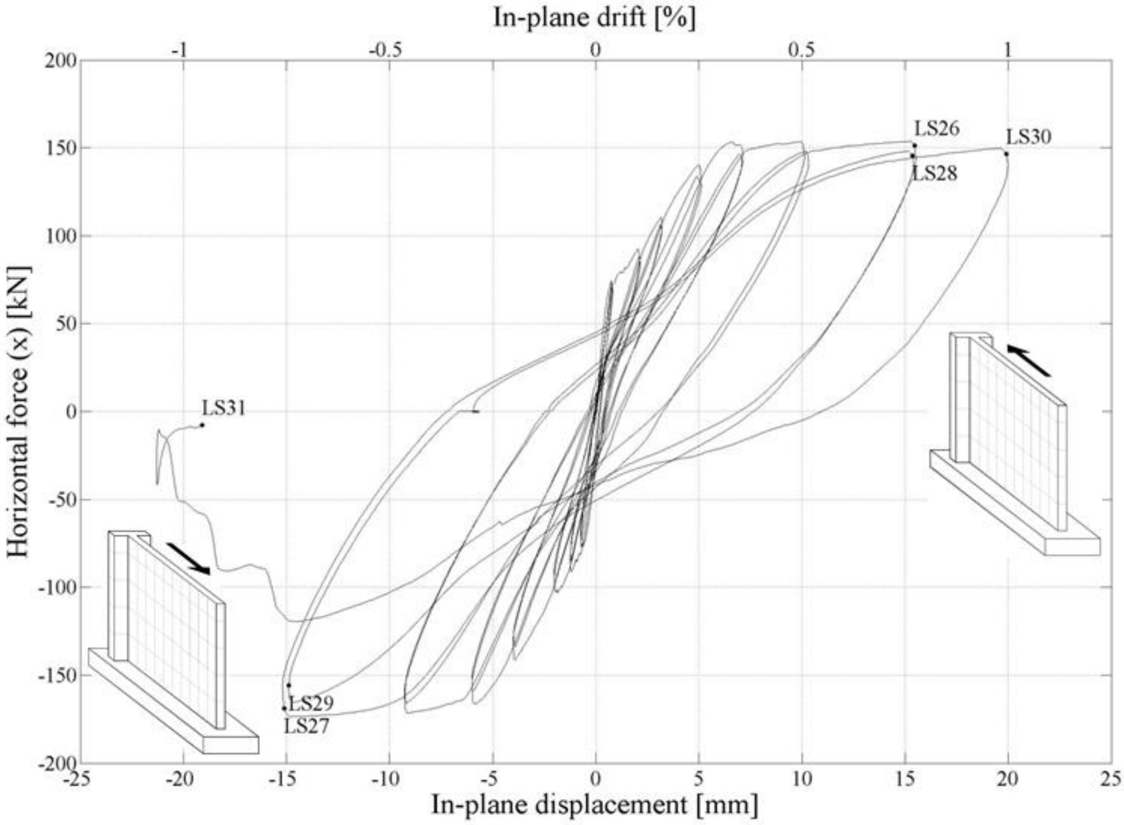

Figure 7. In-plane force-displacement response of wall TW1.

(a)

(b)

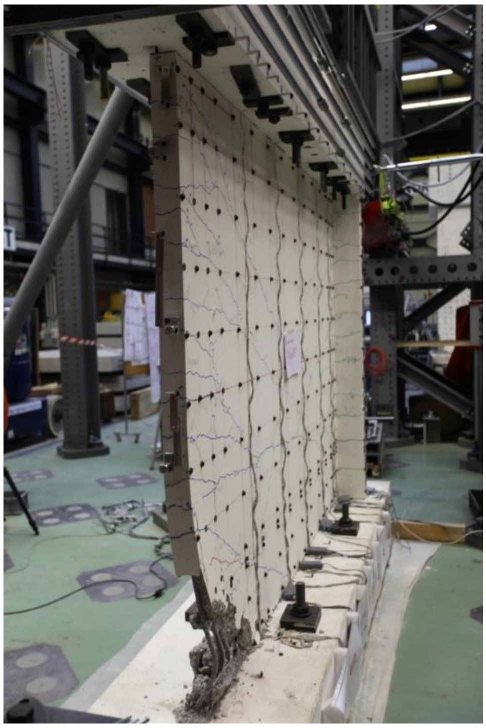

Figure 8. (a) Deformed shape of the wall at loading LS30→LS31 (around 0% in-plane drift);
(b) At the end of the test, after failure.

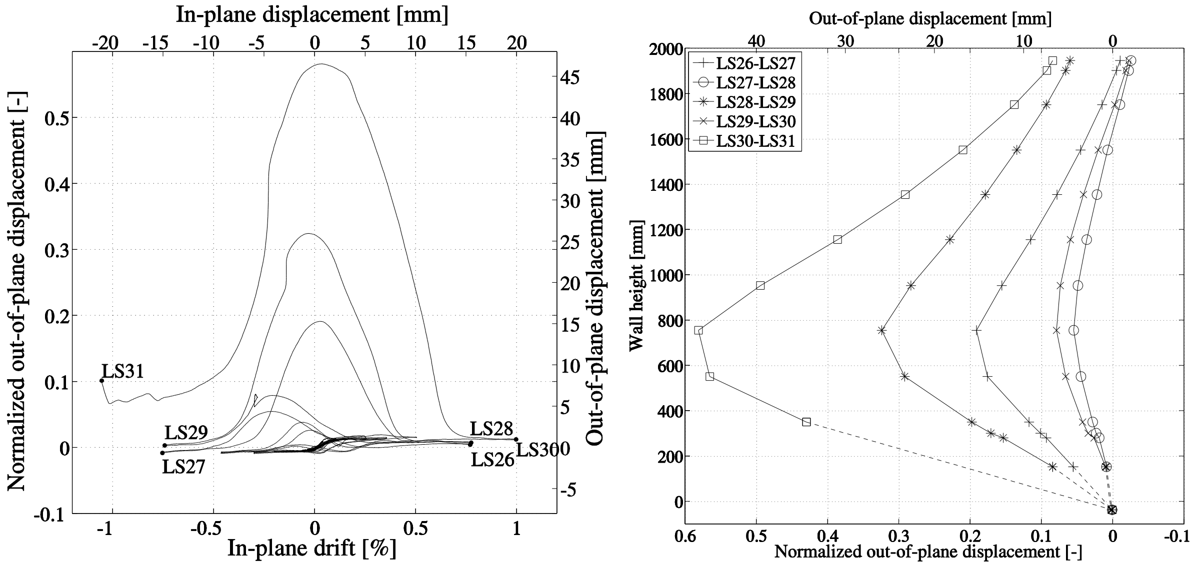

Figure 9. (a) Imposed in-plane drift versus normalized web edge maximum out-of-plane displacement as obtained with LED #7; (b) Normalized web edge out-of-plane displacement profile along the wall height between consecutive load stages.

Bearing the above in mind, a qualitative description of the failure mechanism may be stated as follows. During loading LS30→LS31, following the occurrence of evident out-of-plane deformations visible in Figure 8(a) and the progression of concrete crushing, a local buckling of the longitudinal rebars in the bottom part of the boundary element at the free web edge took place. Post-failure observations indicate that the reinforcing bar with d_b = 16 mm closer to the web edge buckled more than the second rebar, and this one more than the third rebar in the boundary element. More importantly, it can be seen that the buckling of the rebars, as shown in Figure 8(b), occurs in the opposite direction to that of the wall overall buckled configuration depicted in Figure 8(a). Such phenomenon can be ascribed to the fact that, in the out-of-plane direction, the wall bottom/top connections to the foundation/RC beam can be more closely assimilated to fixed-fixed boundary conditions than to the pinned-pinned case. Therefore, the maximum out-of-plane moments at the extremities are expected to be of opposite sign than that at the wall mid-height, and of a larger absolute value. Figure 9(b) hints at such a reverse curvature near the top and bottom of the wall. The occurrence of buckling at the wall base and not at its top is naturally related to the in-plane moment gradient, which is larger at the base.

Member failure was hence clearly promoted by wall instability, which also aggravated concrete crushing and local out-of-plane reinforcement buckling. In other words, although the collapse of the member occurred at a local level, it was mainly triggered by the development of a global mode of deformation.

5. NEW FINDINGS

The observations of the experimental results are currently compared to the hypotheses on which existing models are based that predict the out-of-plane behaviour of RC walls. These models are the model by Paulay and Priestley [7] and Chai and Elayer [8]. Based on the obtained test results, an ongoing effort investigates in particular the following points:

- *Normalized out-of-plane displacements:* Paulay and Priestley [7] postulated that an upper bound for failure by out-of-plane buckling is the occurrence of lateral out-of-plane displacements δ exceeding half of the wall thickness b_w, i.e., when ξ=0.5. They also assumed that, in a real structure, failure should occur at a smaller eccentricity and hence from the equilibrium considerations of section 2.1 the stability criterion of eq. (2) was derived. Later, the same criterion was used by Chai and Elayer [8]. The wall TW1 attained, however, a maximum normalized out-of-plane displacement above 0.5 (ξ_{max}=0.57 at LED #7, as evidenced in Figure 9). The ongoing work investigates the influence of assumed rebar strains and boundary conditions on the maximum out-of-plane displacement that can be reached.

- *Part of the wall that develops out-of-plane displacements:* Concerning the height l_0 along which out-of-plane buckling develops, it has been suggested [7,8] that, since large strains may be expected only over the lower part of the plastic region, l_0 can be taken as the equivalent plastic hinge length l_p. Besides, it should be less than 80% of the clear unsupported height of the wall, h_w. For TW1, computing the buckling length as proposed by Paulay and Priestley [7], one obtains that $l_0=l_p=0.20l_w+0.044h_w$=628mm. From Figure 9(b), however, it can be observed that out-of-plane deformations involve roughly the entire wall height, i.e., $h_b=h_w$, and also the entire wall length while the small flange restrains at that end the wall from developing significant out-of-plane deformations.

- *Influence of the tensile strain on the out-of-plane behaviour:* The maximum tensile strain has been recognized as the critical parameter influencing the lateral stability of walls in the literature [7,8]. The ongoing work aims at developing a model that links it explicitly to the prediction of the maximum out-of-plane displacement.

6. CONCLUSIONS

Following a review of the out-of-plane wall buckling mechanics and current modelling techniques, the present paper described an experimental test of a thin RC wall loaded only in its own plane. Despite using only one layer of longitudinal reinforcement along the wall length, cyclic lateral load resistance of the wall was satisfactory up to ±0.75% drift. During cycling to -1% drift, the wall experienced lateral instability and failed in a brittle manner. Given the small lateral drift capacity, it is obvious that the wall details used in accordance with the Colombian design practice is not suitable in high seismic regions if the expected wall drift is above 0.75%.

The measured out-of-plane deformations were significant and allowed to obtain a series of new findings and question commonly accepted hypotheses. Namely, the wall attained a yet unseen normalized out-of-plane displacement larger than half the section thickness, while optical measurements showed that the buckling zone covers roughly the entire storey height and is hence not limited to the predicted plastic hinge region. The restraining effect of the tensioned part of the wall was evident, and the relevance of the maximum tensile strain as a critical parameter to evaluate the vulnerability to instability was confirmed. Besides, it seems possible to relate this value to the attained maximum out-of-plane displacement. The previous conclusions should be used to update and adjust the existing phenomenological models and to develop, tune and compare finite elements of distinct levels of complexity.

ACKNOWLEDGMENTS

The authors would like to thank Prof. Carlos Blandon (School of Engineering of Antioquia, Colombia) and Prof. Ricardo Bonett (University of Medellin, Colombia) for designing the test specimen TW1. The test specimen was constructed and tested at EPFL with a Seed money grant from EPFL. The help of Jose Rave Arango and the entire staff of the structural engineering laboratory during wall testing is gratefully acknowledged.

REFERENCES

[1] J.W. Wallace, L.M. Massone, P. Bonelli, J. Dragovich, R. Lagos, C. Lüders, et al., Damage and Implications for Seismic Design of RC Structural Wall Buildings, Earthq. Spectra. 28 (2012) S281–S299.

[2] F. Dashti, R.P. Dhakal, S. Pampanin, Simulation of out-of-plane instability in rectangular RC structural walls, in: Second Eur. Conf. Earthq. Eng. Seismol., Istanbul, 2014: pp. 1–12.

[3] M. Saatcioglu, D. Palermo, A. Ghobarah, D. Mitchell, R. Simpson, P. Adebar, et al., Performance of reinforced concrete buildings during the 27 February 2010 Maule (Chile) earthquake, 40 (2013) 693–710.

[4] K.J. Elwood, Performance of concrete buildings in the 22 February 2011 Christchurch earthquake and implications for Canadian codes, Can. J. Civ. Eng. 40 (2013) 759–776.

[5] J.W. Wallace, Performance of structural walls in recent earthquakes and tests and implications for US building codes, in: Proceedings15th World Conf. Earthq. Eng., Lisboa, Portugal, 2012.

[6] S. Sritharan, K. Beyer, R.S. Henry, Y.H. Chai, M. Kowalsky, D. Bull, Understanding poor seismic performance of concrete walls and design implications, Earthq. Spectra. 30 (2014) 307–334.

[7] T. Paulay, M.J.N. Priestley, Stability of ductile structural walls, ACI Struct. J. 90 (1993) 385–392.

[8] Y.H. Chai, D.T. Elayer, Lateral stability of reinforced concrete columns under axial reversed cyclic tension and compression, ACI Struct. J. 96 (1999) 780–789.

[9] W.J. Goodsir, The design of coupled frame-wall structures for seismic actions, 1985.

[10] T. Paulay, W.J. Goodsir, The ductility of structural walls, Bull. New Zeal. Natl. Soc. Earthq. Eng. 18 (1985) 250–269.

[11] C.A.P. para el R. de C.S. Colombia: Ministerio de Ambiente, Vivienda y Desarrollo Territorial, NSR-10: Reglamento Colombiano de Constructión Sismo Resistente, Bogotá D.C., 2010.

[12] NDI, Optotrak Certus HD, Northern Digital Inc., (2009).

[13] J.P. Almeida, O. Prodan, A. Rosso, K. Beyer, Tests on thin reinforced concrete walls subjected to in-plane and out-of-plane cyclic loading, 2014.